

# Stress Relaxation and Elastic Moduli in the Swollen and the Shrunk Phases of *N*-Isopropylacrylamide Gel

Shunsuke Hirotsu†

Graduate School of Bioscience and Biotechnology, Tokyo Institute of Technology, Nagatsuta-cho, Yokohama, Kanagawa 226-8501, Japan

Received January 5, 2004; Revised Manuscript Received February 18, 2004

**ABSTRACT:** Stress relaxation has been measured on *N*-isopropylacrylamide gel around the volume phase transition point. In the swollen phase, a uniaxial stretching of the gel induces appreciable swelling, and the kinetics of stress relaxation is identical to that of swelling. In the shrunken phase, the stress relaxation is governed by shear relaxation without swelling. The drastic change in the relaxation kinetics occurs within  $\pm 0.2$  °C of the transition temperature. The results are analyzed in terms of the phenomenological theory of the stress effect on gels and the formal theory of elastic relaxation. Highly contrastive behaviors of the shear relaxation modulus between the two phases have been observed, which indicate that the time scale of the conformation change associated with the shear deformation is much faster in the swollen phase than in the shrunken phase. Possible mechanisms of the stress relaxation in both phases have been proposed.

## 1. Introduction

Volume phase transition of polymer gels has been studied extensively over the past two decades.<sup>1,2</sup> It is now clear that this phase transition, characterized by a large and discontinuous change of the swelling degree at a specific temperature, is a consequence of phase separation between polymer network and solvent. The basic molecular mechanism responsible for the transition is essentially the same as that of phase separation in a corresponding polymer solution, but the presence of a three-dimensional network structure gives some interesting features to the phase transition of gels. The elastic property around the transition is a typical example.

As viewed from a general aspect of solid-state phase transformation, the volume phase transition of gels belongs to elastic phase transition, in which a solid becomes unstable against a particular mode of macroscopic deformation. In gels, the homogeneous volume strain goes unstable, leading to a discontinuous change of the network swelling degree. This instability manifests itself as a divergence of the isothermal osmotic compressibility or, in other words, vanishing of the equilibrium osmotic bulk modulus. The previous study<sup>3</sup> on the static elastic properties of poly(*N*-isopropylacrylamide) gels (abbreviated as NIPA gels) in the vicinity of the transition point has revealed a clear evidence of such elastic instability at the transition. (The elastic moduli treated in the present article are osmotic moduli. For simplicity, however, the adjective “osmotic” will be omitted hereafter.)

In general, the experimentally observed elastic response of a material depends on the relative magnitude between the characteristic time of the measuring technique and the elastic relaxation time of that material.<sup>4</sup> If the former is much shorter than the latter, the measured response is an adiabatic one, while in the opposite limit the quantity measured is an isothermal one. In between these extremes, the measured response

is neither adiabatic nor isothermal but is of intermediate character. In polymer networks, the change from the adiabatic to the isothermal response represents a process of equilibration of chain conformation, and it will contain valuable information on the structure and dynamics of the network.

Around the volume phase transition, the equilibrium composition of a gel changes drastically as a function of temperature. In NIPA gel,<sup>5</sup> for example, the volume fraction of polymer increases from less than 5% to more than 60% as the gel transforms from the swollen to the shrunken phase.<sup>2,6</sup> The large change in the swelling degree will necessarily lead to that of chain conformation and also to various properties of the network. So far, however, detailed study of the relaxation behavior as a function of swelling degree has not been undertaken in any gel. Thus, in the present study, I have measured the elastic relaxation of NIPA gel around the phase transition to elucidate how the nature of the relaxation changes with the swelling degree.

The format of the present paper is as follows. In section 2, the background of the present study is given. In section 3, the experimental method is described with emphases on the construction of the measuring apparatus and the method of sample setting. The results of the measurement are given in section 4, and they are analyzed in section 5 in terms of the phenomenological theory of stress effect in gels and the formal treatment of the elastic relaxation of solid. In section 6, the molecular mechanism of the stress relaxation is considered in relation to the network structure in both phases.

## 2. Background

**2.1. Previous Studies on the Stress Relaxation of Polymer Networks.** Physical properties of a polymer network depend essentially on whether the network is free from solvent or is in contact with solvent, and in the latter case, the quality of solvent is crucial. A solvent-free network is a compact solid, where the degrees of freedom of each chain are highly restricted. A network in contact with good solvent swells to a large

† Now retired. Current address: 4-9-3 Wakamatshu-cho, Fuchu, Tokyo 183-0005, Japan. E-mail shirotsu@jcom.home.ne.jp.

extent becoming soft and fragile, where a relatively large space for motion is available around each chain. A network in contact with poor solvent shrinks to a compact form, but its structure may not necessarily be the same as that of a solvent-free network because some solvent molecules can be incorporated into chains, as typified by bound water in globular proteins.

Historically, elastic relaxation of polymer networks has been studied almost exclusively on solvent-free systems such as cross-linked rubbers.<sup>4</sup> According to these studies, a characteristic feature of the stress relaxation of polymer networks is the presence of an extremely long tail in the relaxation function. For example, Chasset and Thirion<sup>7</sup> measured the stress relaxation of rubber vulcanizates and found that the tension for long times follows closely the power-law formula as

$$X(t) = X_{\text{eq}}[1 + (t/\tau)^{-\gamma}] \quad (1)$$

where  $t$  is time,  $X(t)$  is the uniaxial tension at constant elongation,  $X_{\text{eq}}$  is its equilibrium value, and the parameters  $\tau$  and  $\gamma$  depend on the cross-link density.

Ferry<sup>4</sup> noted that the power law is an excellent representation for mechanical relaxation of various polymer networks and supposed that a possible presence of dangling chains in a network may be responsible for the long-lasting relaxation. Even when the network is kept in a deformed state, a dangling chain can relax to its unperturbed conformation due to movement of its free end, becoming elastically ineffective. This idea was later developed by Curro and Pincus<sup>8</sup> by incorporating the reptation scheme proposed by deGennes.<sup>9</sup> They showed, under some assumptions, that the reptation of dangling chains leads to the power-law relaxation.

Elastic relaxation has also been studied in glassy polymeric solids such as polycarbonates, which, though not permanently cross-linked, also show very long relaxation. For example, LeGrund et al.<sup>10</sup> measured the stress relaxation of glassy bisphenol-A polycarbonate and observed a very long tail in the relaxation function. They found that the result fits closely the KWW formula as

$$X(t) = X_{\text{eq}} + \Delta X \exp[-(t/\tau)^\beta] \quad (2)$$

where  $\beta$  is a positive constant less than unity. Also, Ngai et al.<sup>11</sup> and Bendler et al.<sup>12</sup> found that the stress relaxation in glassy polymeric solids can be represented well by the KWW formula and derived eq 2 from phenomenological models.

In contrast to solvent-free networks, studies on the elastic relaxation of gels are scarce. Takigawa et al.<sup>13</sup> studied the stress relaxation of swollen gels in terms of the equation of motion of a polymer network. Their conclusion was that the stress relaxation obeys the same kinetics as that of swelling. However, their formulation seems to apply only to a special situation where a gel in the relaxed state, i.e., an as-prepared gel, is stretched and not to a general case of stretching an arbitrarily swollen gel.

The stress relaxation of NIPA gel has been measured by Sasaki and Koga.<sup>14</sup> They found that the relaxation in the shrunken phase follows the power law and interpreted the result in terms of the Curro–Pincus theory<sup>8</sup> described above. As for the relaxation in the

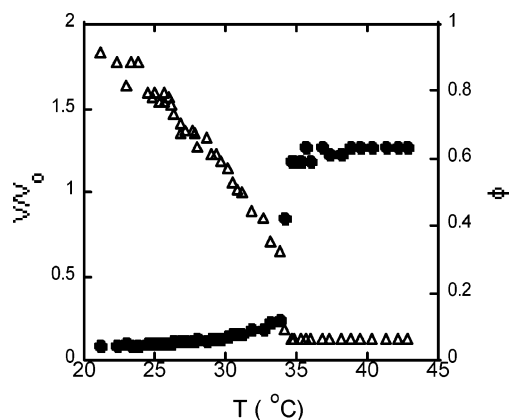


**Figure 1.** Normalized volume  $V/V_0$  (triangles) and volume fraction of polymer  $\phi$  (dots) of NIPA gels in equilibrium with outer water phase as functions of temperature.

swollen phase, they suggested a possible connection between the relaxation and water diffusion.

**2.2. Essentials of the Volume Phase Transition of NIPA Gel.** As some fundamental characteristics associated with the volume phase transition of NIPA gel are prerequisite for a proper understanding of the present work, a brief summary of them will be given below. Figure 1 shows the swelling curves of NIPA gel in equilibrium with outer water phase.<sup>2,6,15,16</sup> Both the normalized volume  $V/V_0$  and the volume fraction of polymer  $\phi$  are plotted against temperature  $T$ , where the subscript 0 refers to the value in the relaxed state of the network or, in other words, the value when the network was synthesized. It is seen that the gel volume decreases (concentration of polymer increases) as temperature rises, and at 33.6 °C which we designate as  $T_0$ , it drops abruptly down to about only 10% of the value at 25 °C. A careful measurement reveals a slight discontinuity of the volume at this temperature,<sup>2,6,15,16</sup> which is an indication of a first-order phase transition. In contrast to the low-temperature swollen phase, the volume in the high-temperature shrunken phase is nearly independent of temperature.

To understand the nature of this transition, it is instructive to know the relative number of monomeric unit of NIPA and water molecules contained in the gel. By a simple calculation using the measured  $\phi(T)$  together with the molecular weight and the density of the constituents, we can obtain the number of water molecules per monomeric unit of NIPA,  $W(T)$ , as

$$W(T) = \frac{M_N}{M_W} \frac{\rho_W}{\rho_N} \left[ \frac{1 - \phi(T)}{\phi(T)} \right] \quad (3)$$

Here,  $M$  is the molecular weight,  $\rho$  is the density, and the subscripts N and W refer to NIPA and water, respectively.

The result is shown in Figure 2. It is seen that there are about 140 water molecules per NIPA monomer around 20 °C, but the number decreases as temperature rises, and at the transition it drops discontinuously down to about 4. It has often been stated<sup>17</sup> that a gel is a kind of solution where a solid network is dissolved in a bulk water phase. The swollen phase of NIPA gel conforms to this view, but it is surely not the case for the shrunken phase. Rather, it is natural to consider that water molecules remaining in the shrunken phase are bound to hydrophilic groups in the network. Thus, the shrunken NIPA is more like a plasticized solid

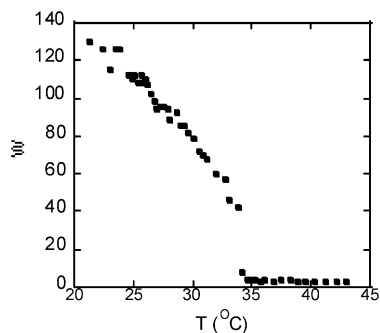


**Figure 2.** Number of water molecules per monomeric unit of NIPA contained in NIPA gel as a function of temperature.

network rather than gels in the usual sense. The above result shows clearly that the volume phase transition of NIPA gel is a phase separation between the network and solvent.

Although physical as well as physicochemical studies on NIPA gels have been developed extensively, almost all of them are on the swollen phase, leaving various properties of the shrunken phase unknown. This is mostly due to the difficulty encountered in preparing good, homogeneous samples of shrunken gel. From the viewpoint of phase transition study, the present status is clearly undesirable because information from only one side of the transition is available. In this connection, to study some fundamental properties in the shrunken phase is one of the aims of the present study.

### 3. Experimental Section

**3.1. Preparation of Gel.** Samples were thin gel rods with the diameter at the time of gelation equals to 1.0 mm. Gels were synthesized by radical copolymerization in an aqueous solution containing 700 mM NIPA and 8.6 mM cross-linker *N,N*-methylenebis(acrylamide) (BIS). As the method of preparation was the standard one which has been described in many places,<sup>3,5,15,16</sup> it will not be repeated here. In the present experiment, gel rods prepared were cut into pieces of 50–70 mm long and then dried completely. Drying was inevitable to fix the gel to tips of the sample holder, as will be explained below.

**3.2. Measuring System.** An elastometer for fragile gels has been constructed in the present study. In particular, it was so designed that the measurement is possible on a sample kept in water. The elastometer comprises an electronic balance (Sartorius A.G., A200S), an electrically driven translation stage, an aquarium, a sample holder, a horizontal microscope with a video recording system, and a computer. The balance must be of such a type as having a hanging hook beneath its base, to which a glass tip holding a gel sample can be attached. The tensile force imposed on the gel can be measured with the balance to within  $\pm 10^{-4}$  gram-force, i.e.,  $9.81 \times 10^{-7}$  N.

A block diagram of the apparatus is shown in Figure 3. The whole system is constructed on a steel frame (L) placed on a vibration-free base. The sample gel rod (D) is held vertically between the upper (C) and the lower (E) tips, both of which are made of glass capillaries. The upper tip is connected to a hanging hook (B) of the electronic balance (A), and the lower one is secured to the base plate of the sample holder (H), which is placed at the center of a rectangular glass sample cell (F). The sample cell is placed in an aquarium (G), which has flat transparent glass windows through which the sample can be continuously monitored and recorded with a horizontal microscope equipped with a video camera (K). The magnification of the microscope can be changed from  $\times 30$  to  $\times 10$  depending on the purpose of measurement. The volumes of the sample cell and the aquarium are about 20 cm<sup>3</sup> and 700 cm<sup>3</sup>, respectively. The aquarium is set on the electrically driven Z-stage (Z), with which the vertical separation between the

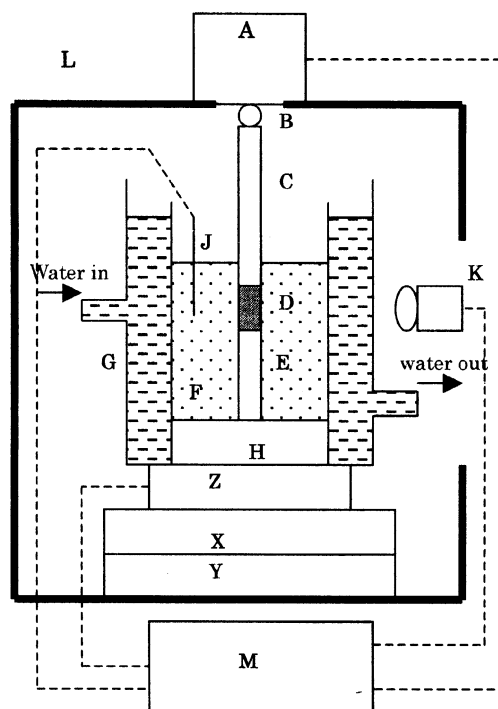


**Figure 3.** Block diagram of the elastometer: (A) electronic balance, (B) hanging hook, (C) upper tip, (D) (shown dark) gel rod, (E) lower tip, (F) sample cell, (G) outer aquarium, (H) base plate of the sample holder, (J) thermocouple, (K) horizontal microscope with a video camera, (L) (bold line) steel frame, (M) personal computer, (X, Y) manual translation stage in the two horizontal directions, (Z) electric translation stage in the vertical direction. Inside G and F (both textured) are filled with temperature-controlled water and distilled water, respectively. Dashed lines represent cables for signal transmission.

upper and the lower tips can be adjusted to within  $\pm 2$   $\mu$ m. In addition to the Z-stage, there are two manual X- and Y-stages, with which the position of the lower tip can be adjusted in the horizontal plane such that the two tips and the gel rod lie on a vertical line. Note that the parts above the gel, i.e., A, B, and C, are fixed, while those below it, i.e., E, F, G, and H, can be shifted as one body with respect to the upper portion by manipulation of the X, Y, and Z stages.

After the dried gel is fixed between the tips (see the next subsection for the method of fixing), distilled water is injected into the sample cell F, and temperature-controlled (within  $\pm 0.05$  °C) water is circulated between the aquarium G and the water bath (not shown). Temperature is monitored with a thermocouple (J) placed near the sample. Numerical values of the tensile force imposed on the sample are sent from the balance to the computer (M) at a constant rate and saved in a text file as a function of time. In addition, the temperature of water around the gel and the vertical position of the stage Z are also saved. At the same time, the microscopic image of the sample is recorded with the video microscope. The time is also superposed on videotape, so that image of the gel and other numerical data are recorded on the common time base, from which the stress relaxation and the elastic moduli can be calculated.

**3.3. Method of Fixing a Gel Rod.** The most delicate point in the present measuring technique is how to fix an extremely fragile, thin gel rod between the upper and the lower tips. The fully swollen gel rods with this thin were so fragile that it was impossible to manipulate them with tweezers or by any other means without breaking them. For this reason, I first fixed a dried gel between the glass tips and then let the gel swell by injecting water into the sample cell. It has already been confirmed<sup>3,18</sup> that drying and reswelling of NIPA gels do not give observable influence on their swelling and phase transition properties. Details of fixing a gel rod between the tips are shown in Figure 4. The tips (C and E) are Pyrex glass



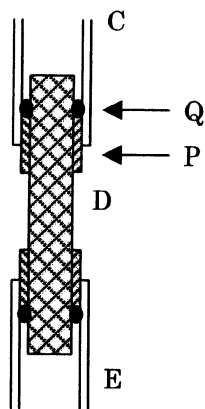


**Figure 4.** Connection between a gel rod and capillaries: (C) upper capillary, (D) (crosshatched) gel rod, (E) lower capillary, (P) (hatched) silicone tubing, (Q) (dark) silicone adhesive.

capillaries with the internal diameter 1.2 mm. Soft silicone rubber tubes (P) serve as a mechanical buffer between the gel (D) and the inner wall of the capillary. Without these cushions, repeated elongation and contraction of the gel, which are inevitable in the present measurement, surely damage the gel at contact points between the gel and the ends of the capillaries.

The diameter of the capillary, that of the silicone tube, and that of the gel rod have to be so chosen that they fit tightly with each other so that they do not slip with each other under tension. To be concrete, the inner diameter of the glass capillary should be slightly smaller than the outer diameter of the silicone tube, and the inner diameter of the silicone tube should be slightly smaller than the equilibrium diameter of the gel rod at 30.0 °C. In the shrunken phase, however, the diameter of the gel becomes smaller than that of the silicone tube so that the gel will slip under tension against the tube. To prevent this, both ends of the gel are glued with soft silicone adhesive (Q, Bath-Bond, Konishi, Inc.) to the inner surfaces of the capillaries.

After the sample is fixed in position, distilled water is injected into the sample cell, and the gel swells to equilibrium within a few days. During this period, the length of the gel increases by about three times. If the positions of the upper and the lower tips are fixed, the gel certainly breaks in the very early stage of swelling. To prevent this, it is absolutely necessary to adjust the separation between the upper and the lower tips in such a way that it always matches the natural length of the gel. In this apparatus, this can be accomplished by automatic control of the position of the lower tip as will be explained below.

**3.4. Computer Control.** Two control modes are available in the present system, i.e., the constant-length mode and the constant-force mode. In the former, the separation between the tips is kept constant, and the force imposed on the gel is continuously recorded. This mode enables us to measure the stress relaxation and the elastic moduli.

In the latter mode, the separation between the tips is automatically adjusted so as to keep the tension at a constant value, which is usually chosen nearly equal to zero. As was described above, this mode is inevitable to bring a dried gel fixed between the tips into swelling equilibrium. This mode is also absolutely necessary when the temperature of the sample is changed. Without adjusting the separation between the tips, the gel will surely break when it changes the swelling degree according to the change of temperature. Before the measurements, the gel was kept still under the control of constant-force mode (zero tension) for at least 24 h to establish the swelling equilibrium.

**3.5. Measurement Procedure.** Two conditions that are prerequisite for reliable measurements were checked before the measurements. The first concerns the stability of the measuring apparatus. Because the stress relaxation of gel takes a long time, and the force to be measured is very small,

it is crucial to keep the performance of the measuring apparatus as constant as possible during the duration of measurement. Sometimes, nonnegligible background drift of the force was observed even after the gel attained equilibrium, but in appropriate cases the background was stable over a long enough period of time. The primary cause of the background drift was identified to be the change in environmental temperature because intimate correlation was found between the former and the latter. The thermal expansion or contraction of the glass tips, of the brass base plate, and of the aluminum translation stages should change the distance between the tips, thereby altering the force imposed on the sample. Thus, the temperature surrounding the apparatus must be kept as constant as possible. The measurements were started only after the background settled within  $\pm 2$  mg-weight per hour. The drift of this level gives inaccuracy of 0.5% at most to the stress relaxation data.

The second condition is that the linearity between the stress and the strain must hold so that we can calculate the elastic moduli from the stress-strain relation. For our gel, Hooke's law was found to be satisfied within  $\pm 0.1\%$  as long as the strain is smaller than 0.2, which is below the deformation limit of the present measurements.

The actual measurement proceeded as follows. After the gel attained swelling equilibrium, the constant-force mode was stopped and the Z-stage was lowered to such a position that the magnitude of the shift was 5–20% of the total length (typically the shift was between 0.5 and 3.0 mm). At the same time, the constant-length mode was switched on, and the data were sent to the computer at a programmed time interval (usually every 2–10 s). The microscopic images of the sample were recorded on videotape throughout the measurement.

A weak point of the present apparatus is that it cannot measure accurately the instantaneous response. With our motor-driven translation stage, it took at least 1 s or so to change the vertical position of the stage by 1 mm or so. Thus, the data obtained within a first few seconds were less accurate than the rest of the data. Although this can be improved somewhat by using a faster translation stage, it will in principle be difficult to measure the adiabatic response by static stress-strain measurements.

**3.6. Data Reduction.** The length and the diameter of the gel rod were measured on video microscopic images using an image analysis software. It is particularly important to measure the length and the diameter of the gel at exactly the same position of the sample throughout a single run. Actually, the measured length was not the total length between the tips but the distance between a pair of tiny scars or slight irregularities on the surface of the gel near the center of the length. Although tiny scars or irregularities are often introduced accidentally in the course of gelation, if no such visible marks are found, the sample had to be replaced with a new one until an appropriate one is met. The diameter was measured in the same region as the length was measured. The accuracy of these measurements was well within  $\pm 5$   $\mu\text{m}$ .

The tension due to stretching,  $X(t)$ , is equal to the tensile force  $F(t)$  divided by the cross-sectional area  $S(t)$  of the sample, viz.

$$X(t) = \frac{F(t)}{S(t)} \quad (4)$$

Let the length and the diameter just before stretching be  $L(0)$  and  $D(0)$ , respectively, and those at time  $t$  after stretching be  $L(t)$  and  $D(t)$ , respectively. We define the displacements of the length and the diameter by the following equations.

$$\delta L(t) = L(t) - L(0) \quad (5)$$

$$\delta D(t) = D(t) - D(0) \quad (6)$$

In the linear range, Young's modulus  $Y$ , the bulk modulus  $K$ , the shear modulus  $\mu$ , and Poisson's ratio  $\sigma$  are written respectively as follows.

$$Y = \frac{X}{\delta L/L(0)} \quad (7)$$

$$K = \frac{Y}{3(1 - 2\sigma)} \quad (8)$$

$$\sigma = -\frac{\delta D/D(0)}{\delta L/L(0)} \quad (9)$$

$$\mu = \frac{Y}{2(1 + \sigma)} \quad (10)$$

In the above equations, all the quantities except  $L(0)$  and  $D(0)$  are functions of time, though time dependence is not written explicitly. The time-dependent modulus is called the elastic relaxation modulus,<sup>4</sup> which tends to the equilibrium modulus in the long-time limit. We will henceforth use the subscript eq to denote the equilibrium modulus.

#### 4. Results

The measurements were made at various temperatures between 28.0 and 40.0 °C on a number of different samples. Among the results obtained, some typical ones will be presented below for the swollen phase, the shrunken phase, and the transition region.

**4.1. Changes of Diameter and Volume Induced by Stretching.** In Figure 5, the diameter and the volume of the gel rod are plotted as functions of time after stretching for both phases. In the swollen phase at 30 °C, which is 3.6 °C below  $T_0$ , a sudden stretching of 12% ( $\delta L/L(0) = 0.12$ ) induced an instantaneous decrease of the diameter of about 5.6% followed by a gradual recovery, and after about  $7 \times 10^3$  s, it almost settled to a value that was smaller than the value before stretching by about 2.6%. The volume of gel changed little just after stretching and then increased gradually, settling eventually to a value larger than that before stretching by about 6.1%. This indicates clearly that the stretching induced swelling. In the shrunken phase at 35.0 °C, a stretching of 17% induced an instantaneous decrease of the diameter by 7.5% and an increase of the volume by 0.7%, both of which changed little thereafter; i.e., the stretching scarcely induced swelling.

**4.2. Stress Relaxation in the Swollen and the Shrunken Phases.** In the swollen phase, we must regard both  $F(t)$  and  $S(t)$  as time dependent in calculating eq 4. At 30.0 °C, for example, the cross-sectional area of the rod increases about 6% during 7500 s. In the shrunken phase, on the other hand, we can safely assume that the cross-sectional area is constant after the stretching as is evident from Figure 5b. The stress relaxation thus calculated is shown in Figure 6 for both phases. Because of the difference in the data processing mentioned above, the scatter of the data points is larger in Figure 6a than in Figure 6b.

In the swollen phase, it is noticeable that the stress relaxation is similar to the diameter relaxation, as is inferred from visual comparison of Figures 5a and 6a. This suggests that the kinetics of stress relaxation is intimately related to that of swelling. Later, we will see this is indeed the case through theoretical consideration and curve fitting. In the shrunken phase, as is clear in Figure 6b, the initial relaxation is much faster than in the swollen phase, and it is followed by a long tail. This behavior is reminiscent of a transition from glasslike to rubberlike responses seen in rubber networks.<sup>4</sup>

**4.3. Stress Relaxation in the Transition Region.** Results in the close vicinity of the transition are shown

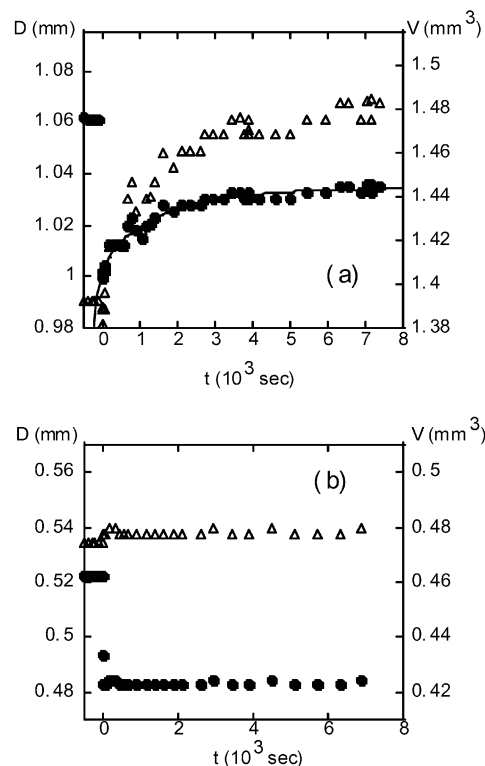


**Figure 5.** Diameter  $D$  (dots) and volume  $V$  (triangles) of NIPA gel rod at 30.0 °C (a) and at 35.0 °C (b) as functions of time. The instant at which the gel was abruptly stretched is taken as the origin of time. The solid line in (a) is the best-fit result to the Li-Tanaka formula.

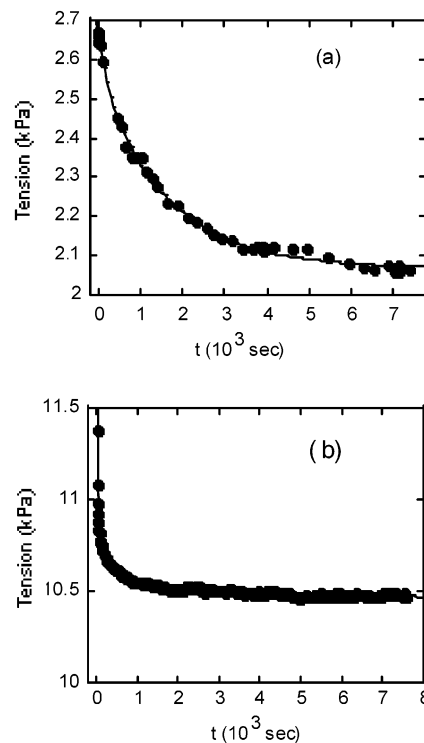


**Figure 6.** Stress relaxation of NIPA gel rod at 30.0 °C (a) and at 35.0 °C (b). The solid lines are the best-fit results to the Li-Tanaka formula (a) and to the power law (b).

in Figure 7. It is seen that the drastic change of the relaxation function occurs in the close vicinity of  $T_0$ , i.e.,  $T_0 \pm 0.2$  °C, and the curve is apparently irregular just at  $T_0$ . This is due to the coexistence of the two phases at the first-order phase transition,<sup>2,6,15,16</sup> which

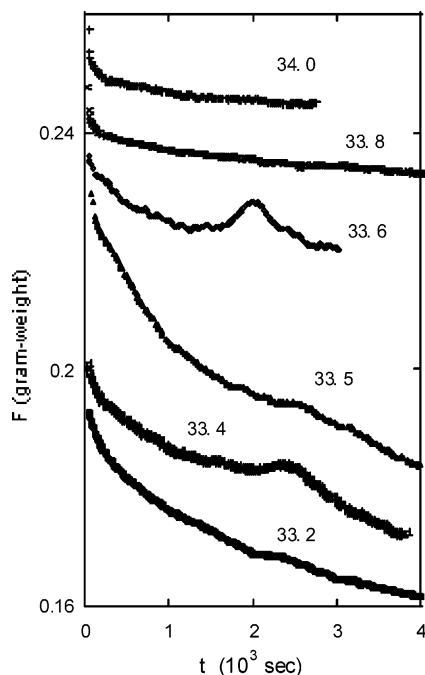


**Figure 7.** Change in stress relaxation of NIPA gel as it traverses the transition point,  $T_0 = 33.6$  °C, from the low-temperature side. Numerals denote temperatures in °C. The values on the ordinate are for the lowermost curve, and those for other curves are shifted appropriately for clarity.

**Table 1. Equilibrium Moduli of NIPA Gel at 30.0 °C (Swollen Phase) and at 35.0 °C (Shrunken Phase)<sup>a</sup>**

$T$ (°C)	$Y_{eq}$ ( $\times 10^4$ Pa)	$K_{eq}$ ( $\times 10^4$ Pa)	$\mu_{eq}$ ( $\times 10^4$ Pa)	$\sigma_{eq}$
30.0	$1.85 \pm 0.04$ ( $1.8^b$ , $1.5^c$ )	$1.1 \pm 0.2$ ( $1^b$ )	$0.76 \pm 0.03$ ( $0.8^b$ )	$0.21 \pm 0.02$ ( $0.2^b$ )
35.0	$5.87 \pm 0.11$ ( $4.2^d$ , $10^c$ )	$12 \pm 10$ ( $10^d$ )	$2.07 \pm 0.08$ ( $2^d$ )	$0.42 \pm 0.03$ ( $0.43^d$ )

<sup>a</sup> Values in parentheses are literature values, which are read out by the present author from graphs in the respective publications and thus should be regarded as approximate values. <sup>b</sup> Measured at 33.0 °C. Hirotsu, S. *J. Chem. Phys.* **1991**, *94*, 3949. <sup>c</sup> The amount of cross-linker is about 20% larger than our gel. Sasaki, S.; Koga, S. *Macromolecules* **2002**, *35*, 857. <sup>d</sup> Measured at 34.5 °C. Hirotsu, S. *J. Chem. Phys.* **1991**, *94*, 3949.

makes the gel macroscopically inhomogeneous. The curves at 33.4 and 33.5 °C also show some irregularities, which may suggest that nuclei of the shrunken phase already emerged at these temperatures. It has been known<sup>18</sup> that the application of tension shifts the transition temperature upward, but the amount of the shift due to the tension used in the present measurement is estimated<sup>18</sup> to be well below 0.1 °C.

#### 4.4. Elastic Moduli and Elastic Relaxation Moduli.

To calculate the equilibrium moduli, the equilibrium values of the tension and the diameter are necessary. These were estimated in two ways. First, the measured values in the long-time region (7000–7600 s) were averaged. Second, the long-time limits were taken in the best-fit formulas to be discussed later. These two methods yielded values that coincided with each other well within  $\pm 0.5\%$ . The moduli thus calculated are given in Table 1 together with the already reported ones. The error limits shown in Table 1 has been estimated on the basis of the fact that the errors in  $L$  and  $D$  are within  $\pm 5$   $\mu\text{m}$ , as has been described before. The exceptionally large error in  $K_{eq}$  at 35 °C is due to the fact that  $K_{eq}$  is extremely sensitive to the value of  $\sigma_{eq}$  when the latter is near 0.5, i.e.,  $dK/d\sigma \sim (1 - 2\sigma)^{-2}$ .

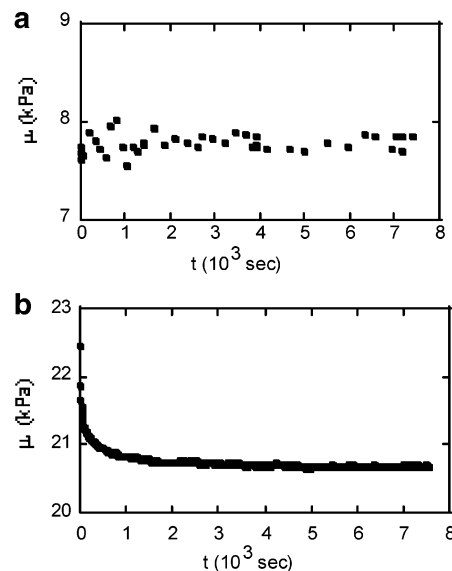


**Figure 8.** Shear relaxation modulus of NIPA gel at 30.0 °C (a) and at 35.0 °C (b).

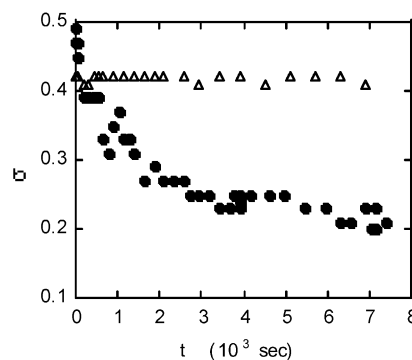


**Figure 9.** Relaxation of Poisson's ratio of NIPA gel at 30.0 °C (dots) and at 35.0 °C (triangles).

The relaxation moduli have been calculated with eqs 7–10. As can be easily seen from these equations,  $Y(t)$  is proportional to  $X(t)$ , and  $K(t)$  in the shrunken phase is proportional to  $Y(t)$ . The relaxation of  $K(t)$  in the swollen phase is enhanced by that of  $\sigma(t)$ . Other relaxation moduli,  $\mu(t)$  and  $\sigma(t)$ , are shown in Figures 8 and 9, respectively, both of which are interesting in the present context, and will be referred to later in the Analysis section.

It is seen that the shear modulus in the swollen phase (Figure 8a) is almost constant with little relaxation, whereas that in the shrunken phase (Figure 8b) exhibits clear relaxation that is quite similar to the stress relaxation (Figure 6b). As is clear in Figure 9, Poisson's ratio shows clear relaxation in the swollen phase, but it is almost constant in the shrunken phase.

## 5. Analysis

### 5.1. Equilibrium of Gels under Uniaxial Tension.

We have seen above that the stretching of gel induces further swelling in the swollen phase, whereas such effect is absent in the shrunken phase. Moreover, it seems that the stress relaxation in the swollen phase is intimately related to the swelling. Thus, it will be important in the present context to understand the origin of the stretch-induced swelling and also the reason why this occurs only in the swollen phase but not in the shrunken phase. These can be interpreted in

terms of the phenomenological theory of the stress effect on gels,<sup>18</sup> the outline of which will be given below.

According to the theory of gel swelling due originally to Flory,<sup>17</sup> the Gibbs free energy of a freely swollen gel can be expressed as follows.

$$\Delta G \equiv G - G_1 = k_B T \{ N_s [\ln(1 - \phi) + \chi\phi] + \frac{3}{2} N_c (\alpha^2 - \ln \alpha - 1) \} \quad (11)$$

Here,  $G$  is the Gibbs free energy of a gel containing  $N_c$  chains and  $N_s$  solvent molecules,  $G_1$  is the sum of free energies of solvent and amorphous solid polymer,  $\chi$  is the solvent–polymer interaction parameter,  $k_B$  is the Boltzmann constant, and  $\alpha$  is the linear swelling ratio defined as

$$\alpha \equiv (V/V_0)^{1/3} = (\phi_0/\phi)^{1/3} \quad (12)$$

The equilibrium condition of gel is

$$(\partial \Delta G / \partial \alpha)_T = 0 \quad (13)$$

So far, we have been considering a homogeneous and isotropic gel. Applying a uniaxial tension to such a gel makes it anisotropic. In analogy with the isotropic case, we can specify the anisotropic swelling by two swelling ratios,  $\alpha_{||}$  and  $\alpha_{\perp}$ , which are defined using the length and the diameter of the gel rod as

$$\alpha_{||} = L/L_0 \quad (14)$$

$$\alpha_{\perp} = D/D_0 \quad (15)$$

where  $L_0$  and  $D_0$  refer to the length and the diameter of the gel rod when it was synthesized. The free energy of a gel under uniaxial tension can be obtained by adding the work term to  $G$  as

$$\Delta G = k_B T \left\{ N_s [\ln(1 - \phi) + \chi\phi] + \frac{N_c}{2} (\alpha_{||}^2 + 2\alpha_{\perp}^2) - \frac{1}{2} N_c \left[ \ln \left( \frac{\phi_0}{\phi} \right) + 3 \right] \right\} - FL \quad (16)$$

where  $F$  is the applied tension. Note that the work refers to the relaxed state of the network, not to the swollen state before stretching.

The equilibrium conditions for the uniaxially stretched gel can be expressed as

$$(\partial \Delta G / \partial \alpha_{||})_{T, \alpha_{\perp}} = 0 \quad (17)$$

and

$$(\partial \Delta G / \partial \alpha_{\perp})_{T, \alpha_{||}} = 0 \quad (18)$$

From eqs 17 and 18, we can derive two equations which determine the equilibrium of gel under tension as

$$[\ln(1 - \phi) + \phi + \chi\phi^2 - \phi^2(1 - \phi)(\partial\chi/\partial\phi)] - (v_1 N_c / N_A V_0) [(\phi/2\phi_0) - 1/\alpha_{||}] = 0 \quad (19)$$

and

$$\alpha_{\perp}^2 = \alpha_{||}(\alpha_{||} - \alpha_c) \quad (20)$$

where  $v_1$  is the molar volume of solvent,  $N_A$  is Avogadro's

number, and  $\alpha_c$  is defined by  $\alpha_c \equiv FL_0 / N_c k_B T$ . For derivation of these equations, see the Appendix.

In conventional gels the volume is not sensitive to temperature, and  $\chi$  depends little on polymer concentration. In temperature-sensitive gels, however,  $\chi$  depends significantly on  $\phi$ , and this makes the volume depend strongly on temperature. The origin of the volume phase transition lies, at least in phenomenological terms, in the strong concentration dependence of  $\chi$ .<sup>19</sup> Previous studies<sup>2,3,6</sup> have shown that the swelling and the phase transition in NIPA gels can be reproduced fairly well by even retaining the linear term alone in  $\chi(\phi)$ . Thus, we put

$$\chi(\phi) = \chi_1 + \chi_2 \phi \quad (21)$$

where  $\chi_2$  is a numerical constant and  $\chi_1$  can be written as

$$\chi_1 = (\delta h - T\delta s) / k_B T \quad (22)$$

where  $\delta h$  and  $\delta s$  are the enthalpy and the entropy changes associated with the solvent–polymer contact.<sup>17</sup> These parameters can be determined through fitting the calculated swelling curve to the experimental one.<sup>2,3,6,18</sup>

Numerical calculations in terms of eqs 19–22 show that the volume of gel at 30 °C increases by about 10% due to stretching of about 10%, whereas the volume change due to the same amount of stretching is well below 0.1% at 40 °C. This difference can be understood quite simply as follows. Rewriting eq 19, the equilibrium condition under tension is

$$[\ln(1 - \phi) + \phi + \chi\phi^2 - \phi^2(1 - \phi)(\partial\chi/\partial\phi)] - (v_1 N_c / N_A V_0) [(\phi/2\phi_0) - \xi(\phi/\phi_0)^{1/3}] = 0 \quad (23)$$

where  $\xi = (1 + \delta L/L(0))^{-1}$ . It is seen that the effect of stretching on equilibrium is contained solely in  $\xi$ . In the present experiment,  $\xi$  is not far from unity, i.e., 0.85–1.0. Then, whether the stretching affects appreciably on the equilibrium or not depends on the relative magnitudes between  $(\phi/2\phi_0)$  and  $(\phi/\phi_0)^{1/3}$ . If the latter dominates the former, even a small change of  $\xi$  affects equilibrium, but in the reverse situation,  $\xi$  is of no importance. In the case of NIPA gel at 30.0 °C, the latter is more than 2 times larger than the former, whereas at 35 °C the former is about 1.8 times larger than the latter. These results explain qualitatively the fact that the stretching alters the equilibrium composition of gel in the swollen phase, but not in the shrunken phase.

Both terms  $(\phi/2\phi_0)$  and  $(\phi/\phi_0)^{1/3}$  come from the rubber elasticity, i.e., the change of the entropy due to swelling. Roughly speaking, the former comes from the kinetic freedom associated with the volume of the network and the latter from the change in the distribution of end-to-end distance of chains.<sup>17</sup> Thus, we can say that the origin of the stretch-induced swelling lies in the change in the latter due to stretching. Numerical calculation with eq 23 shows that the stretch-induced swelling occurs only if  $\chi$  is smaller than about 0.51. This clearly shows that the phenomenon of stretch-induced swelling is not inherent to temperature-sensitive gels but is a general feature of swollen gels and that this effect is absent in deswollen gels.

## 5.2. Stress Relaxation in the Swollen Phase.

According to the linear constitutive equations of elasticity, stresses due to externally imposed strains can be



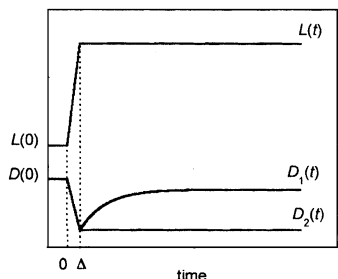


**Figure 10.** Schematic time courses of the length  $L$ , the diameter in the swollen phase  $D_1$ , and that in the shrunken phase  $D_2$ . The interval between 0 and  $\Delta$  is greatly exaggerated for clarity.

expressed in terms of the shear relaxation modulus  $\mu(t)$  and the bulk relaxation modulus  $K(t)$  as follows.<sup>4</sup>

$$X_{ij}(t) = \int_{-\infty}^t \left\{ \mu(t-t') \left[ \dot{S}_{ij}(t') - \frac{1}{3} \sum \dot{S}_{kk}(t') \delta_{ij} \right] + \frac{2}{3} K(t-t') \left[ \frac{1}{3} \sum \dot{S}_{kk}(t') \delta_{ij} \right] \right\} dt' \quad (24)$$

Here,  $X_{ij}$  and  $S_{ij}$  are the stress and the strain tensor components, respectively,  $\delta_{ij}$  is the Kronecker delta, and the dot over  $S$  means the time derivative.

In applying eq 24 to the present experiment, we take the direction of the stretch, which is the direction of the rod axis, as the 1-direction. Then, the uniaxial tension  $X(t)$  can be written as

$$X(t) = X_{11}(t) - X_{22}(t) = \int_{-\infty}^t \mu(t-t') [\dot{S}_{11}(t') - \dot{S}_{22}(t')] dt' \quad (25)$$

With eqs 5 and 6, we can write the strains as

$$S_{11}(t) = \delta L(t)/L(0) \quad (26)$$

and

$$S_{22}(t) = \delta D(t)/D(0) \quad (27)$$

The time courses of the length and the diameter of the rod in the present experiment are depicted in Figure 10. At time  $t = 0$ , the stretching sets in so that both  $S_{11}$  and  $S_{22}$  begin to be induced. At  $t = \Delta$ , they reach  $S_{11}(\Delta)$  and  $S_{22}(\Delta)$ , respectively, and  $S_{11}$  is fixed, there. After  $t = \Delta$ ,  $S_{22}$  is independent of time in the shrunken phase, whereas it relaxes to the new equilibrium value under tension in the swollen phase. Of course, the time interval  $\Delta$  is negligibly short as compared with the duration of the measurement. Assuming that the strains between  $t = 0$  and  $\Delta$  changes linearly with time, we write eq 25 as

$$X(t) = \int_0^\Delta \mu(t-t') \left( \frac{S_{11}(\Delta)}{\Delta} \right) dt' + \int_\Delta^t \mu(t-t') \dot{S}_{11}(t') dt' - \int_0^\Delta \mu(t-t') \left( \frac{S_{22}(\Delta)}{\Delta} \right) dt' - \int_\Delta^t \mu(t-t') \dot{S}_{22}(t') dt' \quad (28)$$

The first and the third integrals on the right-hand side of eq 28 can be approximated using the mean value theorem, and for  $t \gg \Delta$  we obtain

$$X(t) = [S_{11}(\Delta) - S_{22}(\Delta)]\mu(t) + \int_\Delta^t \mu(t-t') \dot{S}_{11}(t') dt' - \int_\Delta^t \mu(t-t') \dot{S}_{22}(t') dt' \quad (29)$$

The second term of the right-hand side of eq 29 vanishes, and the third term can be rewritten using partial integration to obtain

$$X(t) = [S_{11}(\Delta) - S_{22}(\Delta)]\mu(t) - [\mu(0)S_{22}(t) - \mu(t)S_{22}(\Delta)] + \int_\Delta^t \mu(t-t') S_{22}(t') dt' \quad (30)$$

In the swollen phase,  $\mu(t)$  is almost constant (Figure 8a), so that eq 30 reduces to

$$X(t) = C - \mu(0)S_{22}(t) \quad (31)$$

where  $C$  is a numerical constant. This equation shows that the stress relaxation is identical with the diameter relaxation reversed in sign.

To test the above prediction, I first fitted the diameter relaxation in the swollen phase to the equation derived by Li and Tanaka<sup>20</sup> for the swelling kinetics of long cylindrical gels. Using the graphs given in their paper together with the elastic moduli given in Table 1, we can determine numerical coefficients in the Li–Tanaka formula. The formula with the coefficients thus determined is

$$D(t) = D(0) + B[(0.75 \exp(-t/3.0\tau_s) + 0.1 \exp(-t/0.58\tau_s) + 0.05 \exp(-t/0.25\tau_s))] \quad (32)$$

where  $B$  is the scaling factor and  $\tau_s$  is the relaxation time of the sphere having the same diameter as the rod. The best fit result shown as a solid line in Figure 5a is given by  $D(0) = 1.03$ ,  $B = -0.0360$ , and  $\tau_s = 533$ . Next, I fitted the stress relaxation at 30.0 °C to the same formula as

$$X(t) = X(0) + B[(0.75 \exp(-t/3.0\tau_s) + 0.1 \exp(-t/0.58\tau_s) + 0.05 \exp(-t/0.25\tau_s))] \quad (33)$$

The result shown in Figure 6a is  $X(0) = 2.067$ ,  $B = 0.666$ , and  $\tau_s = 534$ . The best-fit values of  $\tau_s$  in eqs 32 and 33 coincide with each other almost perfectly. Thus, it has been confirmed experimentally that the stress relaxation and the diameter relaxation follow the same kinetics.

**5.3. Stress Relaxation in the Shrunken Phase.** In the shrunken phase, both the second and the third terms of eq 29 can be neglected. We thus obtain

$$X(t) = [S_{11}(\Delta) - S_{22}(\Delta)]\mu(t) \quad (34)$$

This shows that the stress relaxation should be proportional to the shear relaxation modulus, which is in accord with our experimental results. The same conclusion can also be obtained from eqs 7–10 considering that  $\sigma(t)$  is almost constant after stretching.

As has been interpreted in section 2.2, the structure of shrunken NIPA gel seems to be more akin to a solid network than a swollen gel. Thus, I tried to fit the stress relaxation in this phase to eq 1, which has been applied widely to solvent-free networks. As shown in Figure 11, the log–log plot of  $X(t)$  is almost linear, which ensures that the power law is a good approximation. The best-fit curve shown as a solid line in Figure 6b is eq 1 with  $X_{eq} = 10.44$ ,  $\tau = 0.307$ , and  $\gamma = 0.564$ . However, it should



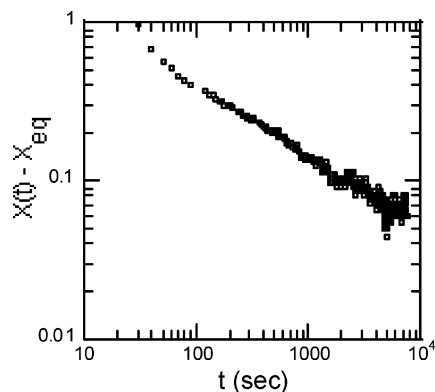


**Figure 11.** A log-log plot of the stress relaxation in the shrunken phase.  $X_{eq}$  is put equal to 10.44, as was estimated from the data in Figure 6b.

also be mentioned that the KWW formula, eq 2, can fit the same data as equally well as the power law does. Because the fitting curve to this formula is almost indistinguishable from the power-law curve shown in Figure 6b, it will not be reproduced here.

**5.4. Elastic Moduli.** In Table 1, the equilibrium moduli determined in the present work are compared with the previous data. Although all these values have been obtained from static stress-strain measurements, details of the measuring techniques are all different. Moreover, the cross-link densities of samples used as well as the temperature at which the measurements were made are not exactly the same with each other. Considering these points, we may say that the agreement among the values is satisfactory.

According to the theory of gel elasticity, the shear modulus can be expressed as<sup>21</sup>

$$\mu_{th} = \nu_0 \left( \frac{\phi}{\phi_0} \right)^{1/3} k_B T \quad (35)$$

where  $\mu_{th}$  stands for the theoretical shear modulus and  $\nu_0$  is the density of cross-links in the relaxed state. Assuming the idealized situation where a perfect network has been formed without any loss of cross-linkers and monomers, we can estimate  $\nu_0$  from the preparation condition. Thus, the right-hand side of eq 33 for our NIPA gel is calculated to be  $2.2 \times 10^4$  Pa at 30.0 °C and  $4.3 \times 10^4$  Pa at 35.0 °C, which are larger than our experimental  $\mu_{eq}$  at corresponding temperatures by 3.0 and 2.1 times, respectively. Such discrepancies between theoretical and experimental moduli have frequently been observed in polymer networks.<sup>4</sup> This is understandable considering that real networks are far from perfect in that they contain dangling chains, entanglements, and sol fractions, and therefore the number of elastically effective chains in a real network should be much smaller than that expected for an ideal one.

Figure 8 demonstrates the sharp contrast in the shear relaxation modulus between the swollen and the shrunken phases. The results indicate that the shear strain in the swollen phase relaxes much faster than the time scale of the present measurement (1 s), and this in turn suggests that the conformation changes associated with the shear deformation are fast local rearrangements of segments that are independent of the large-scale conformation change of the whole network associated with the swelling. The result in the shrunken phase, to the contrary, seems to indicate that the shear strain cannot relax as fast as in the swollen phase. This

is understandable because spatial constraints inherent to the compact structure may preclude fast segmental motion even on a local scale.

## 6. Discussion

The stretch-induced swelling is a unique feature of swollen gels in contact with solvent and is a manifestation of the fact that the thermal and the mechanical equilibria in such systems are inseparably connected with each other. We may hence say that the collective diffusion of the network, which is the molecular process driving the swelling,<sup>22</sup> is also the mechanism underlying the stress relaxation. In deswollen gels, on the other hand, the stretching does not induce swelling, and the stress relaxes via rearrangement of chain conformations occurring under a constant volume. As has been shown above, the stress relaxation of shrunken NIPA gel follows closely the power law, which has been applied widely to solvent-free networks. To explain the stress relaxation in rubbers, some authors<sup>4,8</sup> have proposed a model in which dangling chains play a crucial role in the relaxation process. Unfortunately, the parameters  $\tau$  and  $\gamma$  defined in the theory<sup>8</sup> are complex functions of quantities that cannot easily be estimated such as the length and the distribution of dangling chains, the reptation time, and the density of cross-links. Thus, quantitative comparison between the theory and experiment is difficult.

To the present author's view, it will be premature to apply this model as it stands to our result because the structure of the network will be considerably different between vulcanized rubbers and NIPA gels. In the former, cross-links are introduced between a pair of long strands in solvent-free condition, which results in a compact network. In the latter, to the contrary, both the polymerization and the cross-linking reactions proceed simultaneously in an aqueous solution of monomers of NIPA and BIS, giving rise to a swollen network. In addition, unlike natural rubbers, NIPA has a large side chain. Average molecular weight of chains between a pair of adjacent cross-links calculated from the Flory-Huggins formula<sup>7,17</sup> is about 3 times larger in our NIPA gels than that reported for rubbers.<sup>7</sup> From these considerations, I suspect that not only dangling chains but also mechanical constraints among network chains, which have been neglected in the previous theory,<sup>4,8</sup> will be important in our gels.

In this context, it is noteworthy that the KWW formula can fit our result as equally satisfactorily as the power law does. Although it is true that eq 2 essentially coincides with the power law when either  $\tau \gg t$  or  $\beta \ll 1$  is satisfied,<sup>23</sup> the present case conforms to neither of these conditions, and thus the above result is not trivial. There have been a number of attempts to derive the KWW formula from microscopic theoretical models for polymers<sup>24,25</sup> as well as for general disordered systems.<sup>26,27</sup> Above all, it seems to the present author that a key concept of the structural relaxation in polymer gels is a hierarchical structure in the temporal domain,<sup>26,27</sup> from which the KWW relaxation law naturally emerges. For example, in a hierarchically constrained dynamics model<sup>27</sup> developed for glassy systems, various degrees of freedom (DoF) are divided into a series of levels in such a way that DoF in a higher (slower) level can relax only when some of the DoF in an adjacent lower (faster) level acquires the right configuration. This picture seems to conform well to the

kinetics of conformation change induced by external stimulus in a polymer network. Although application of this idea to actual gels will necessitate more information on the structure of the gel network, it would be worthwhile trying to understand the network dynamics and kinetics of gels in terms of the hierarchical relaxation.

Finally, it should be noted that the stretch-induced swelling, a characteristic feature of swollen gels in contact with solvent, cannot occur if the swollen gel under deformation is isolated from solvent. The stress relaxation of gels that is free but not in contact with solvent will be quite different from and possibly much faster than that of gels in contact with solvent. Thus, measurement of the stress relaxation on such gels as a function of the swelling degree will be interesting to study how the extent of free space around each chain influences the kinetics of conformation change.

## 7. Summary

The kinetics of stress relaxation of NIPA gels is found to be quite different between the swollen and the shrunken phases. In the former, the stress relaxation is governed by the volume relaxation due to swelling, whereas in the latter, the stress relaxation is a shear relaxation without volume change. However, the mechanism of relaxation in the shrunken phase may not necessarily be the same as that of rubbers because the network structure of hydrogels may be significantly different from that of rubbers. Further studies, both experimental and theoretical, on the stress relaxation of swollen and deswollen hydrogels will give valuable insight into the dynamics and kinetics of polymer networks.

**Acknowledgment.** The author is grateful to Professor T. Okajima for enlightening discussion on the shear modulus of gels.

## Appendix

Derivation of eqs 19 and 20 from eqs 16–18 is as follows. The right-hand side of eq 16 can be divided into the isotropic part  $\Delta G_i$  and the anisotropic one  $\Delta G_a$  as

$$\Delta G = \Delta G_i(\phi) + \Delta G_a(\alpha_{\parallel}, \alpha_{\perp})$$

where

$$\Delta G_i(\phi) = k_B T \left\{ N_s [\ln(1 - \phi) + \chi\phi] - (N_c/2) [\ln(\phi_0/\phi) + 3] \right\}$$

$$\Delta G_a(\alpha_{\parallel}, \alpha_{\perp}) = k_B T (N_c/2) (\alpha_{\parallel}^2 + 2\alpha_{\perp}^2) - F(L - L_0)$$

The equilibrium condition eq 17 can be executed as

$$(\partial \Delta G / \partial \alpha_{\parallel})_{T, \alpha_{\perp}} = (\partial \Delta G_i / \partial \phi)_T (\partial \phi / \partial \alpha_{\parallel})_{T, \alpha_{\perp}} + (\partial \Delta G_a / \partial \alpha_{\parallel})_{T, \alpha_{\perp}}$$

Thus, we obtain

$$k_B T \left\{ \frac{N_s}{\phi(\phi - 1)} [\ln(1 - \phi) + \chi\phi] + N_s \left( \chi - \frac{1}{1 - \phi} + \phi \frac{\partial \chi}{\partial \phi} \right) + \frac{N_c}{2\phi} \right\} - N_c k_B T \alpha_{\perp}^2 + FL = 0 \quad (\text{A1})$$

where use has been made of the relation  $\phi_0/\phi = \alpha_{\parallel}\alpha_{\perp}^2$

and also the one derived from the conventional lattice model,  $\phi = xN_c/(N_s + xN_c)$ , where  $x$  is the average number of segments per chain. Similarly, eq 18 becomes

$$k_B T \left\{ \frac{N_s}{\phi(\phi - 1)} [\ln(1 - \phi) + \chi\phi] + N_s \left( \chi - \frac{1}{1 - \phi} + \phi \frac{\partial \chi}{\partial \phi} \right) + \frac{N_c}{2\phi} \right\} - N_c k_B T \alpha_{\perp}^2 = 0 \quad (\text{A2})$$

Equations A1 and A2 are the explicit forms of the equilibrium conditions for the uniaxially stretched gel, but the physical significance of the equations is not clear as they stand. Subtracting side by side of eqs A1 and A2 gives eq 20. Adding side by side of the same equations and using eq 20 together with the relation  $N_s = (N_A V_0/v_1)(\phi_0/\phi)(1 - \phi)$  gives eq 19. Equation 19 specifies the equilibrium volume fraction of the gel under tension, whereas eq 20 the extent of the anisotropic deformation induced by the tension.

## References and Notes

- (1) For a review, see: *Adv. Polym. Sci.* Vols. 109 and 110; *Responsive Gels: Volume Phase Transitions I and II*; Dusek, K., Ed.; Springer: Berlin, 1993.
- (2) Hirotsu, S. *Phase Transitions* **1994**, 47, 183–240.
- (3) Hirotsu, S. *J. Chem. Phys.* **1991**, 94, 3949–3957.
- (4) Ferry, J. D. *Viscoelastic Properties of Polymers*; John Wiley & Sons: New York, 1980.
- (5) Hirokawa, Y.; Tanaka, T. *J. Chem. Phys.* **1984**, 81, 6379–6380.
- (6) Hirotsu, S. In *Adv. Polym. Sci.* Vol. 110; *Responsive Gels: Volume Phase Transitions*; Dusek, K., Ed.; Springer: Berlin, 1993.
- (7) Chasset, R.; Thirion, P. *Proceedings of the Conference on Physics of Non-Crystalline Solids*; Prins, J. A., Ed.; North-Holland: Amsterdam, 1965; p 345.
- (8) Curro, J. G.; Pincus, P. *Macromolecules* **1983**, 16, 559–562.
- (9) de Gennes, P.-G. *Scaling Concept in Polymer Physics*; Cornell University Press: Ithaca, NY, 1979.
- (10) Legrand, D. G.; Olszewski, W. V.; Bendler, J. T. *J. Polym. Sci., Polym. Phys. Ed.* **1987**, 25, 1149–1152.
- (11) Ngai, K. L.; Rendell, R. W.; Yee, A. F.; Bankert, R. J. *Polym. Prepr.* **1985**, 26, 83–84.
- (12) Bendler, J. T.; Shleginger, M. *Macromolecules* **1985**, 18, 591–592.
- (13) Takigawa, T.; Urayama, K.; Morino, Y.; Masuda, T. *Polym. J.* **1993**, 25, 929–937.
- (14) Sasaki, S.; Koga, S. *Macromolecules* **2002**, 35, 857–860.
- (15) Hirotsu, S. *J. Phys. Soc. Jpn.* **1987**, 56, 233–242.
- (16) Hirotsu, S. *J. Chem. Phys.* **1988**, 88, 427–431.
- (17) Flory, P. J. *Principles of Polymer Chemistry*; Cornell University Press: Ithaca, NY, 1953.
- (18) Hirotsu, S.; Onuki, A. *J. Phys. Soc. Jpn.* **1989**, 58, 1508–1511.
- (19) Erman, B.; Flory, P. J. *Macromolecules* **1986**, 19, 2342–2353.
- (20) Li, Y.; Tanaka, T. *J. Chem. Phys.* **1990**, 92, 1365–1371.
- (21) Onuki, A. In *Adv. Polym. Sci.* Vol. 109; *Responsive Gels: Volume Phase Transitions*; Dusek, K., Ed.; Springer: Berlin, 1993.
- (22) Tanaka, T.; Hocker, L.; Benedek, G. B. *J. Chem. Phys.* **1978**, 59, 5151–5159.
- (23) Matsuoka, S. *Polym. J.* **1985**, 17, 321–335.
- (24) Bahar, I.; Erma, B.; Fytas, G.; Steffen, W. *Macromolecules* **1994**, 27, 5200–5205.
- (25) de Gennes, P. G. *Macromolecules* **2002**, 35, 3785–3786.
- (26) Shlesinger, M. F.; Klafter, J. In *Fractals in Physics*; Pietronero, L.; Tosatti, E., Eds.; Elsevier Sci. Pub. B. V.: Amsterdam, 1986; pp 393–397.
- (27) Palmer, R. G.; Stein, D. L.; Abrahams, E.; Anderson, P. W. *Phys. Rev. Lett.* **1984**, 53, 958–961.